1-Bit High Accuracy Carrier Phase Discriminators

CHIEH-FU CHANG
RU-MUH YANG
National Space Organization (NSPO)
Taiwan

MING-SENG KAO
National Chiao-Tung University
Taiwan

Asymptotic derivation of traditional 1-bit arctangent phase discriminator (APD) is derived, even though neighboring quantized samples are dependent. The results reveal that high accuracy can be achieved by an APD in low signal-to-noise ratio (SNR) applications using sufficient samples. For high- SNR applications a novel phase discriminator called noise-balanced digital phase discriminator (NB-DPD), which has a complementary asymptotic performance of APD, is proposed to achieve high accuracy. The threshold SNR 2.6 dB that is suggested to identify either APD or NB-DPD is adopted in a specific application. Finally the sampling, quantization, and environmental noise effects on convergence of the asymptotic performance are discussed, and the simulations are provided to verify the analytical results.

Manuscript received August 21, 2009; revised July 19, 2010 and December 7, 2011; released for publication March 5, 2012.

IEEE Log No. T-AES/49/1/944345.

Refereeing of this contribution was handled by J. Morton.

Authors' addresses: C-F. Chang and R-M. Yang, National Space Organization, Department of Electrical Engineering, 8F, Prosperity 1st Road, Hsinchu, 30078, Taiwan, E-mail: (changccccc@gmail.com); M-S. Kao, Department of Communication Engineering, National Chiao-Tung University, Hsinchu 30050, Taiwan.

I. INTRODUCTION

The idea of 1-bit analog-to-digital-conversion (ADC) has been investigated and widely implemented in software-defined receivers and in low power satellite communications due to efficient bitwise processing and avoidance of automatic gain control [1–6]. For carrier recovery an arctangent phase discriminator (APD) is traditionally used since it maximizes the output signal-to-noise ratio (SNR) in analog cases with an additive-white-Gaussian-noise channel [7]. However due to significant 1-bit ADC quantization loss, i.e., degradation ≥ 1.96 dB [4–5], traditional APD may not be a good choice for some applications that require a high accuracy carrier phase, such as attitude determination, radio occultation monitoring, geodesy, and other applications [8–11]. Chang and Kao propose a novel phase discriminator, called digital phase discriminator (DPD), which utilizes the polarity information provided by 1-bit ADC to estimate signal phase in order to avoid the significant 1-bit quantization loss [12]. It has been shown that DPD achieves much higher accuracy than the traditional APD in noiseless or high SNR environments. However DPD does not perform well in noisy environments because of its sensitivity to environmental noise [12, Fig. 5, 13].

In this paper we propose a modified DPD, called noise-balanced digital phase discriminator (NB-DPD), that works well in both noiseless and noisy environments. The collaborative use of APD and NB-DPD is also investigated in order to achieve high accuracy phase estimation in either high SNR cases or low SNR cases. The most relevant prior research is Host-Madsen and Handel's work [14–15]. The frequency estimation problem of 1-bit sampling on a single sinusoid is investigated. Under the assumption of independence between quantized samples, the joint probability density function is derived by the product of the probability functions of each sample. Then the associated Cramer-Rao lower bound can be derived, and the effects of 1-bit sampling and quantization are discussed accordingly. The approach adopted in our work targets phase estimation and considers the dependence between neighboring quantized samples. Moreover a novel phase discriminator NB-DPD is developed, and the associated asymptotic performance is investigated in order to achieve high accuracy phase estimation. In addition, as we consider a limiter as a binary quantizer with infinite samples, several results in the field of limiter phase detector [16–17] can be used to verify the asymptotic results of our work. This becomes clear later.

This paper is organized as follows. First the traditional inphase-quadrature (I-Q) structure APD that uses a 1-bit ADC is investigated, and the

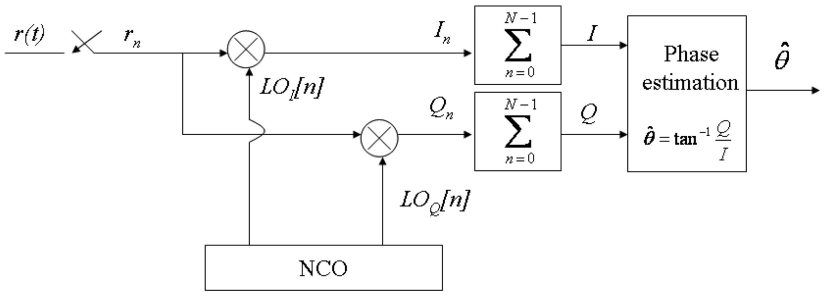

Fig. 1. Phase detection of a 1-bit processing receiver.

stochastic characteristics of each channel correlator output are provided. Then the effects of sampling and 1-bit quantization, as well as asymptotic performance of the APD, are derived. Next a novel phase-discriminator NB-DPD is proposed to attain high accuracy requirements in high SNR cases. The performance of NB-DPD is also provided, and the convergence issue is discussed. The discussion and the conclusion follows.

II. PROBLEM DESCRIPTION OF TRADITIONAL APD

In a 1-bit processing receiver, the traditional approach adopts a APD in the quadrature structure, as shown in Fig. 1. First consider the received signal given by

$$r(t) = \sin(2\pi f_c t + \theta) + u(t) \tag{1}$$

where f_c is the carrier frequency, θ is an unknown phase, and $u(t)$ is the environmental noise. After sampling with 1-bit quantization, the output is represented by

$$r_n = \mathrm{sgn}[\sin(2\pi f_c n T_s + \theta) + u_n] \tag{2}$$

$$= \sin(2\pi f_c n T_s + \theta) + u_n + q_n \tag{3}$$

where $u_n = u[nT_s]$, $\mathrm{sgn}(\cdot)$ denotes the polarity function, and q_n denotes the quantization loss of the nth sample.

Next the local reference signals in Fig. 1 are given by

$$LO_I[n] = \mathrm{sgn}[\sin 2\pi f_{LO} n T_s] \tag{4}$$

$$LO_Q[n] = \mathrm{sgn}[\cos 2\pi f_{LO} n T_s] \tag{5}$$

where f_{LO} is the local carrier frequency. Since the phase estimate is of interest, the local reference frequency f_{LO} is assumed to be equal to the incoming carrier frequency f_c. Then we have

$$\mathbf{I}_n = \mathrm{sgn}[\sin(\phi_n + \theta) + \mathbf{u}_n] \cdot \mathrm{sgn}[\sin\phi_n] \tag{6}$$

$$\mathbf{Q}_n = \mathrm{sgn}[\sin(\phi_n + \theta) + \mathbf{u}_n] \cdot \mathrm{sgn}[\cos\phi_n] \tag{7}$$

where $\phi_n = 2\pi f_c n T_s$. The traditional APD is an arctangent function of the quadrature integration to the inphase integration. Due to quantization loss an asymptotic estimation deviation exists even if $\mathrm{SNR} \to \infty$, and an infinite number of measurement samples are obtained, as shown in Fig. 2. Note that q_n may depend on input signal, and thus the neighboring samples r_ns may be correlated even if noise components u_ns are mutually independent. This feature and the nonlinearity of the sinusoidal function make the derivation of the distribution of $\hat{\theta}$ intractable. In the following we propose an approach that derives the asymptotic deviation of an APD even when considering that the neighboring quantized samples are correlated.

III. DERIVATION OF $E[\mathbf{I}]$ AND $E[\mathbf{Q}]$

First let $f_s = 1/T_s$ be the sampling rate and

$$\frac{f_c}{f_s} = L + \frac{R}{P} \tag{8}$$

where L is the largest integer less than or equal to f_c/f_s while $P > R$, and they are relative prime integers. It has been proved that $(\phi_0, \phi_1 \ldots \phi_{P-1})$ are distributed uniformly over $[0, 2\pi)$ and that $\{\phi_n\}$ are periodic with a period of P, i.e., $\phi_j = \phi_{iP+j}$, where $i, j \in (0, 1, \ldots P-1)$ [12]. These properties are critical in the following derivation. Now we focus on these beginning P samples and define the normalized correlator outputs, given by

$$\mathbf{I} = \frac{1}{P}\sum_{n=0}^{P-1} \mathbf{I}_n \tag{9}$$

$$\mathbf{Q} = \frac{1}{P}\sum_{n=0}^{P-1} \mathbf{Q}_n. \tag{10}$$

Assuming that noise components $\mathbf{u}_0, \mathbf{u}_1 \ldots \mathbf{u}_{p-1}$ are identical, Gaussian, random variables and considering $\phi_n \in [0, \pi)$ in I-channel because $\sin\phi_n > 0$, we have the conditional probabilities given by

$$\Pr(\mathbf{I}_n = 1 \mid \phi_n) = \Pr(\sin(\phi_n + \theta) + \mathbf{u}_n \geq 0 \mid \phi_n)$$

$$= 1 - \mathrm{G}\left(\frac{\sin(\phi_n + \theta)}{\sigma}\right) \tag{11}$$

$$\Pr(\mathbf{I}_n = -1 \mid \phi_n) = \Pr(\sin(\phi_n + \theta) + \mathbf{u}_n < 0 \mid \phi_n)$$

$$= \mathrm{G}\left(\frac{\sin(\phi_n + \theta)}{\sigma}\right) \tag{12}$$

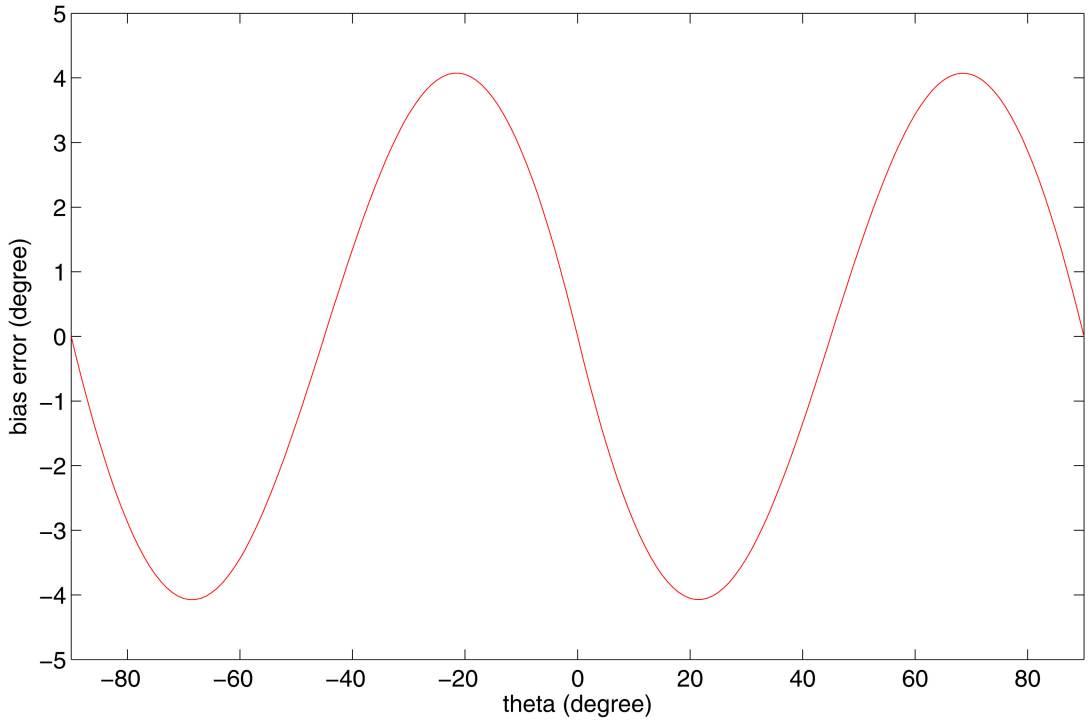

Fig. 2. Asymptotic bias error of APD in 1-bit processing receiver as SNR $\to \infty$.

where σ is the standard deviation of $\mathbf{u}_n$ and where the G-function is defined by

$$\mathrm{G}(z) = \frac{1}{\sqrt{2\pi}} \int_z^{\infty} e^{-x^2/2} dx. \tag{13}$$

Note that $\mathbf{u}_0, \mathbf{u}_1 \ldots \mathbf{u}_{P-1}$ may be dependent in our approach. On the other hand for $\phi_n \in [\pi, 2\pi)$, since $\sin\phi_n \le 0$, the corresponding conditional probabilities are given by

$$\begin{aligned} \Pr(\mathbf{I}_n = 1 \mid \phi_n) &= \Pr(\sin(\phi_n + \theta) + \mathbf{u}_n \le 0 \mid \phi_n) \\ &= \mathrm{G}\left(\frac{\sin(\phi_n + \theta)}{\sigma}\right) \end{aligned} \tag{14}$$

$$\begin{aligned} \Pr(\mathbf{I}_n = -1 \mid \phi_n) &= \Pr(\sin(\phi_n + \theta) + \mathbf{u}_n > 0 \mid \phi_n) \\ &= 1 - \mathrm{G}\left(\frac{\sin(\phi_n + \theta)}{\sigma}\right). \end{aligned} \tag{15}$$

Since $(\phi_0, \phi_1 \ldots \phi_{P-1})$ are deterministic phases and the distributed uniformly over $[0, 2\pi)$, the expected value of $\mathbf{I}$ is given by

$$\begin{aligned} E[\mathbf{I}] &= \frac{1}{P} \sum_{n=0}^{P-1} E[\mathbf{I}_n] \\ &= \frac{1}{P} \cdot \left\{ \sum_{\phi_n \in [0,\pi)} 1 - 2\mathrm{G}\left(\frac{\sin(\phi_n + \theta)}{\sigma}\right) \right. \\ &\qquad \left. + \sum_{\phi_n \in [\pi, 2\pi)} 2\mathrm{G}\left(\frac{\sin(\phi_n + \theta)}{\sigma}\right) - 1 \right\}. \end{aligned} \tag{16}$$

Let $\Delta\phi = 2\pi/p$. When P is sufficiently large, $\Delta\phi \to 0$, and (16) can be rewritten as

$$\begin{aligned} E[\mathbf{I}] &= \frac{1}{P} \cdot \frac{1}{\Delta\phi} \cdot \left\{ \sum_{\phi_n \in [0,\pi)} \left[1 - 2\mathrm{G}\left(\frac{\sin(\phi_n + \theta)}{\sigma}\right)\right] \cdot \Delta\phi \right. \\ &\qquad \left. + \sum_{\phi_n \in [\pi, 2\pi)} \left[2\mathrm{G}\left(\frac{\sin(\phi_n + \theta)}{\sigma}\right) - 1\right] \cdot \Delta\phi \right\} \\ &\approx \frac{1}{2\pi} \cdot \left\{ \int_0^{\pi} \left[1 - 2\mathrm{G}\left(\frac{\sin(\phi + \theta)}{\sigma}\right)\right] \cdot d\phi \right. \\ &\qquad \left. + \int_{\pi}^{2\pi} \left[2\mathrm{G}\left(\frac{\sin(\phi + \theta)}{\sigma}\right) - 1\right] \cdot d\phi \right\} \\ &= \frac{1}{\pi} \cdot \left\{ \int_{\pi}^{2\pi} \mathrm{G}\left(\frac{\sin(\phi + \theta)}{\sigma}\right) d\phi \right. \\ &\qquad \left. - \int_0^{\pi} \mathrm{G}\left(\frac{\sin(\phi + \theta)}{\sigma}\right) d\phi \right\}. \end{aligned} \tag{17}$$

From (1) the SNR of received signal is given by

$$\mathrm{SNR} = \frac{1}{2\sigma^2}. \tag{18}$$

Let $\gamma = \sqrt{2\mathrm{SNR}}$. Then (17) can be simplified as

$$\begin{aligned} E[\mathbf{I}] &= \frac{1}{\pi} \cdot \left\{ \int_{\pi}^{2\pi} \mathrm{G}(\gamma \sin(\phi + \theta)) d\phi \right. \\ &\qquad \left. - \int_0^{\pi} \mathrm{G}(\gamma \sin(\phi + \theta)) d\phi \right\}. \end{aligned} \tag{19}$$

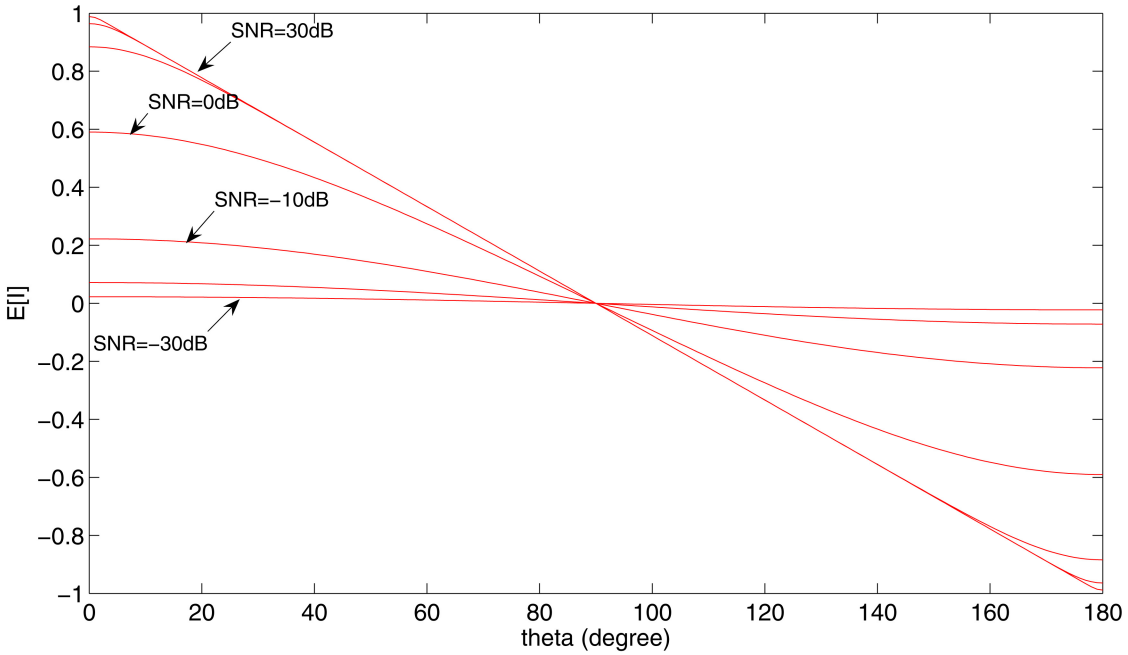

Fig. 3. Expected value of inphase correlator output when SNR = −30 dB, −20 dB…30 dB.

By interchanging variables by $\psi = \phi + \theta$, (19) becomes

$$E[\mathbf{I}] = \frac{1}{\pi} \cdot \left\{ \int_{\pi+\theta}^{2\pi+\theta} \mathrm{G}(\gamma \sin\psi) d\psi - \int_{\theta}^{\pi+\theta} \mathrm{G}(\gamma \sin\psi) d\psi \right\}. \tag{20}$$

From (20) we can derive the expected value of the inphase output for a given θ and SNR. By utilizing (20) we explore the useful properties of $E[\mathbf{I}]$ in the following.

First since $G(a) > G(b)$ if $a < b$, in (20), the maximum of the first term and the minimum of the second term occur when $\theta = 0$ and vice versa when $\theta = \pi$. Hence the maximum of $E[\mathbf{I}]$ occurs at $\theta = 0$, given by

$$E[\mathbf{I}]_{\max} = \frac{1}{\pi} \cdot \left\{ \int_{\pi}^{2\pi} \mathrm{G}(\gamma \sin\psi) d\psi - \int_{0}^{\pi} \mathrm{G}(\gamma \sin\psi) d\psi \right\} \tag{21}$$

and the minimum occurs at $\theta = \pi$, given by

$$\begin{aligned} E[\mathbf{I}]_{\min} &= \frac{1}{\pi} \cdot \left\{ \int_{0}^{\pi} \mathrm{G}(\gamma \sin\psi) d\psi - \int_{\pi}^{2\pi} \mathrm{G}(\gamma \sin\psi) d\psi \right\} \\ &= -E[\mathbf{I}]_{\max}. \end{aligned} \tag{22}$$

For (21) as $\theta = 0$, the desired signal component and the local replica are completely inphased, and hence the maximum is achieved since the polarization inverse of the noise effect is reduced. On the other hand due to the symmetry property of sinusoids, the minimum is achieved as $\theta = \pi$, with the equivalent value and the opposite sign of the maximum, as shown in (22). Note that from (20), $E[\mathbf{I}] = 0$ when $\theta = \pi/2$. Figure 3 shows $E[\mathbf{I}]$ with respect to θ for different SNRs. From Fig. 3 when SNR $\to \infty$, i.e., a noiseless environment, $E[\mathbf{I}]$ approaches a polynomial of degree 1 regarding θ with $E[\mathbf{I}]_{\max} = 1$ and $E[\mathbf{I}]_{\min} = -1$. In a noisy environment when the SNR becomes extremely low, $E[\mathbf{I}]_{\max} \to 0$ and $E[\mathbf{I}]_{\min} \to 0$. Hence the curve of $E[\mathbf{I}]$ approximates the horizontal line. Note that it is sufficient to plot $E[\mathbf{I}]$ over $\theta \in [0, \pi)$ since it is symmetric about $\theta = 0$.

From (7) following the same reasoning as the I-channel, we have

$$E[\mathbf{Q}] = \frac{1}{\pi} \cdot \left\{ \int_{(\pi/2)+\theta}^{(3\pi/2)+\theta} \mathrm{G}(\gamma \sin\psi) d\psi - \int_{(-\pi/2)+\theta}^{(\pi/2)+\theta} \mathrm{G}(\gamma \sin\psi) d\psi \right\}. \tag{23}$$

Similar to $E[\mathbf{I}]$ in (20), we can utilize (23) to explore useful properties of $E[\mathbf{Q}]$. Figure 4 shows $E[\mathbf{Q}]$ with respect to θ for different SNRs using (23). Similar to $E[\mathbf{I}]$ the curve of $E[\mathbf{Q}]$ regarding θ approaches a polynomial of degree 1, while the maximum of $E[\mathbf{Q}]$ occurs at $\theta = \pi/2$ and while the minimum occurs at $\theta = -\pi/2$. Now we are ready to derive the asymptotic performance of the APD.

IV. ASYMPTOTIC DEVIATION OF APD

The traditional APD is given by

$$\hat{\theta}_{\mathrm{APD}} = \tan^{-1} \frac{Q}{I} \tag{24}$$

where $\tan^{-1}(\cdot)$ denotes the arctangent function. In order to derive the asymptotic performance of the APD, suppose that $N = P \times M$ sufficient samples are

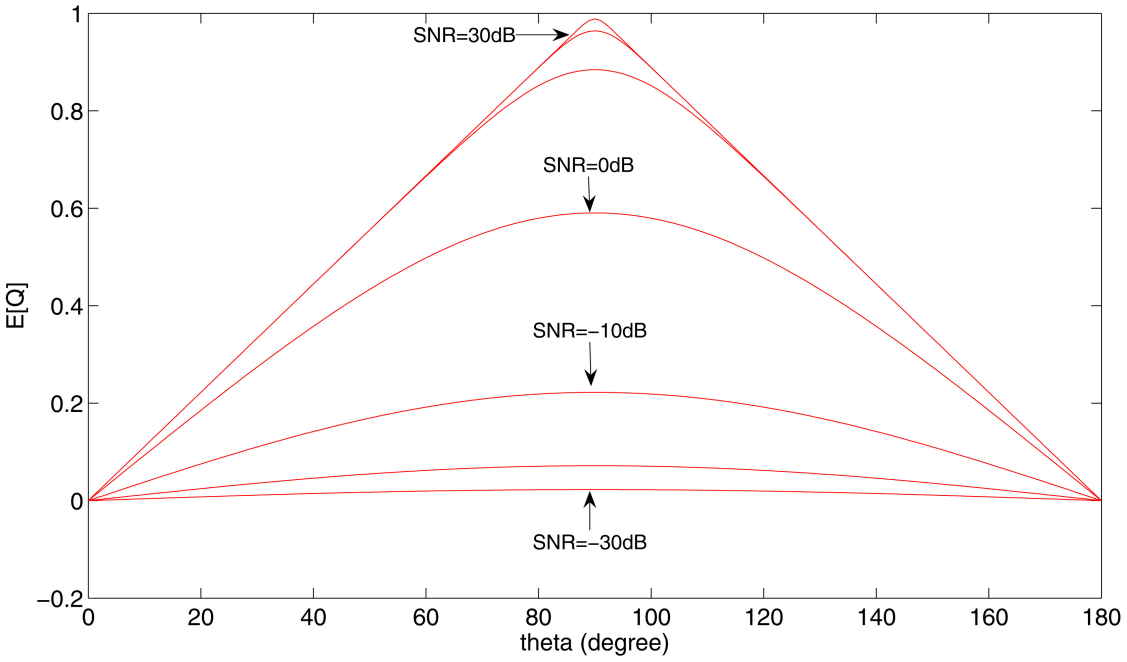

Fig. 4. Expected value of quadrature correlator output when SNR = −30 dB, −20 dB…30 dB.

obtained, where M is an integer. When $\sum_{n=0}^{N-1} I_n \neq 0$ the asymptotic deviation of the APD is given by

$$\lim_{N\to\infty}\hat{\theta}_{\text{APD}} = \tan^{-1}\frac{\lim_{N\to\infty}\frac{1}{N}\sum_{n=0}^{N-1}\mathbf{Q}_n}{\lim_{N\to\infty}\frac{1}{N}\sum_{n=0}^{N-1}\mathbf{I}_n} \tag{25}$$

$$= \tan^{-1}\frac{\lim_{M\to\infty}\frac{1}{PM}\sum_{k=0}^{P-1}\sum_{m=0}^{M-1}\mathbf{Q}_{mP+k}}{\lim_{M\to\infty}\frac{1}{PM}\sum_{k=0}^{P-1}\sum_{m=0}^{M-1}\mathbf{I}_{mP+k}} \tag{26}$$

$$= \tan^{-1}\frac{\frac{1}{P}\sum_{k=0}^{P-1}\lim_{M\to\infty}\frac{1}{M}\sum_{m=0}^{M-1}\mathbf{Q}_{mP+k}}{\frac{1}{P}\sum_{k=0}^{P-1}\lim_{M\to\infty}\frac{1}{M}\sum_{m=0}^{M-1}\mathbf{I}_{mP+k}}. \tag{27}$$

Assume that environmental noise components $\mathbf{u}_n$ and $\mathbf{u}_{n+j}$ are independent when $j \geq P$, where n and j are nonnegative integers. Because $\phi_{iP+k} = \phi_{jP+k}$ for $i \neq j$, every P samples must have the identical phase $\phi_{mP+k} + \theta$, even though θ is unknown, where $m = 0,1,2\ldots M-1$. These sample $\mathbf{I}_{mP+k}$s are independently and identically distributed (IID). This also applies to $\mathbf{Q}_{mP+k}$s. According to the law of large numbers (LLN), we have

$$\lim_{M\to\infty}\frac{1}{M}\sum_{m=0}^{M-1}\mathbf{I}_{mP+k} \to E[\mathbf{I}_k] \tag{28}$$

$$\lim_{M\to\infty}\frac{1}{M}\sum_{m=0}^{M-1}\mathbf{Q}_{mP+k} \to E[\mathbf{Q}_k]. \tag{29}$$

Next since $(\phi_0,\phi_1\ldots\phi_{P-1})$ are distributed uniformly over $[0,2\pi)$ so are $(\phi_0+\theta,\phi_1+\theta\ldots\phi_{P-1}+\theta)$. When P is sufficiently large

$$\frac{1}{P}\sum_{k=0}^{P-1}E[\mathbf{I}_k] \to E[\mathbf{I}] \tag{30}$$

$$\frac{1}{P}\sum_{k=0}^{P-1}E[\mathbf{Q}_k] \to E[\mathbf{Q}] \tag{31}$$

where $E[\mathbf{I}]$ and $E[\mathbf{Q}]$ are given by (20) and (23), respectively. Thus (27) becomes

$$\hat{\theta}_{\text{APD}} \to \tan^{-1}\frac{E[\mathbf{Q}]}{E[\mathbf{I}]} \tag{32}$$

as $N \to \infty$. Notice that the convergence holds even when neighboring quantized samples are dependent. From (20), (23), and (32), the asymptotic deviation of the APD can be derived numerically, as shown in Fig. 5, when -30 dB $\leq$ SNR ≤ 30 dB. From Fig. 5 the asymptotic deviation is a function of θ and the SNR. It exhibits periodic property along θ since the incoming sinusoidal wave is periodic. As SNR$\to\infty$ the maximum estimation error occurs at 21.5°, 68.5°, 111.5°, and 158.5°, while the minimum occurs at 0°, 45°, 90°, and 135°. The maximum deviation is about ±4.1°, and the minimum deviation is zero. The analysis of searching local extrema and the associated positions are provided in Appendix I. Note that the positions of local extrema depend on the SNR and may slightly vary in high SNR cases. Figure 5 also implies that no matter how large the SNR is, the deviation exists even if the sampling count $N \to \infty$. This is illustrated when f_c = 15.42 MHz and when

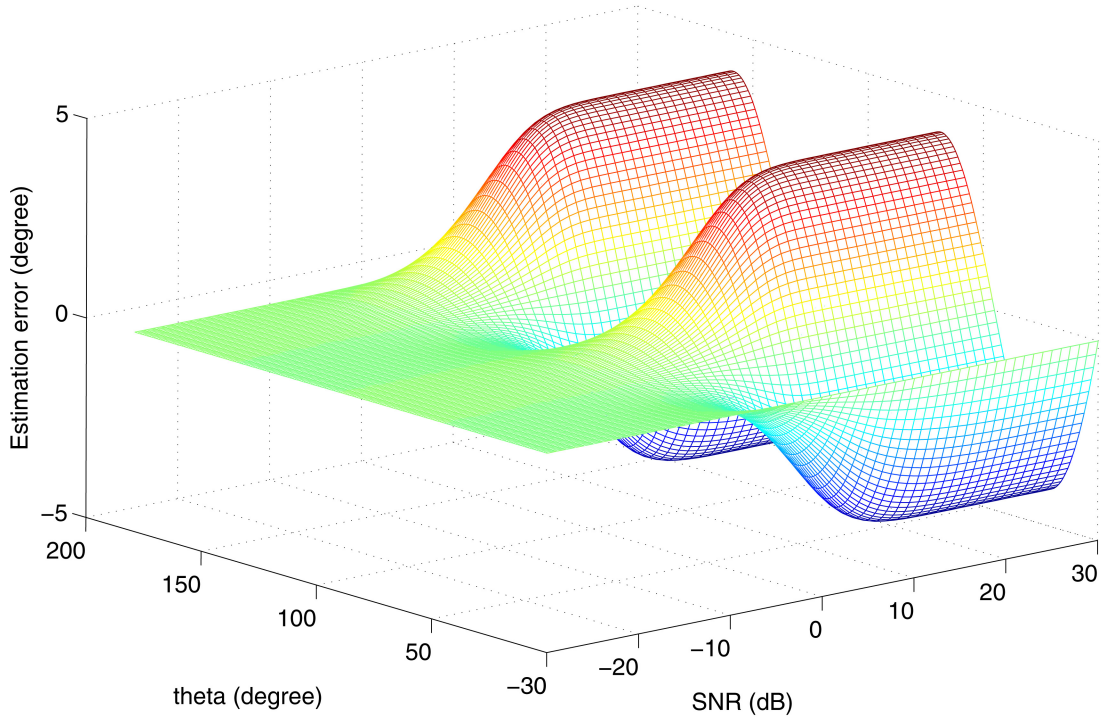

Fig. 5. Asymptotic deviation $\hat{\theta}_{\mathrm{APD}} - \theta$.

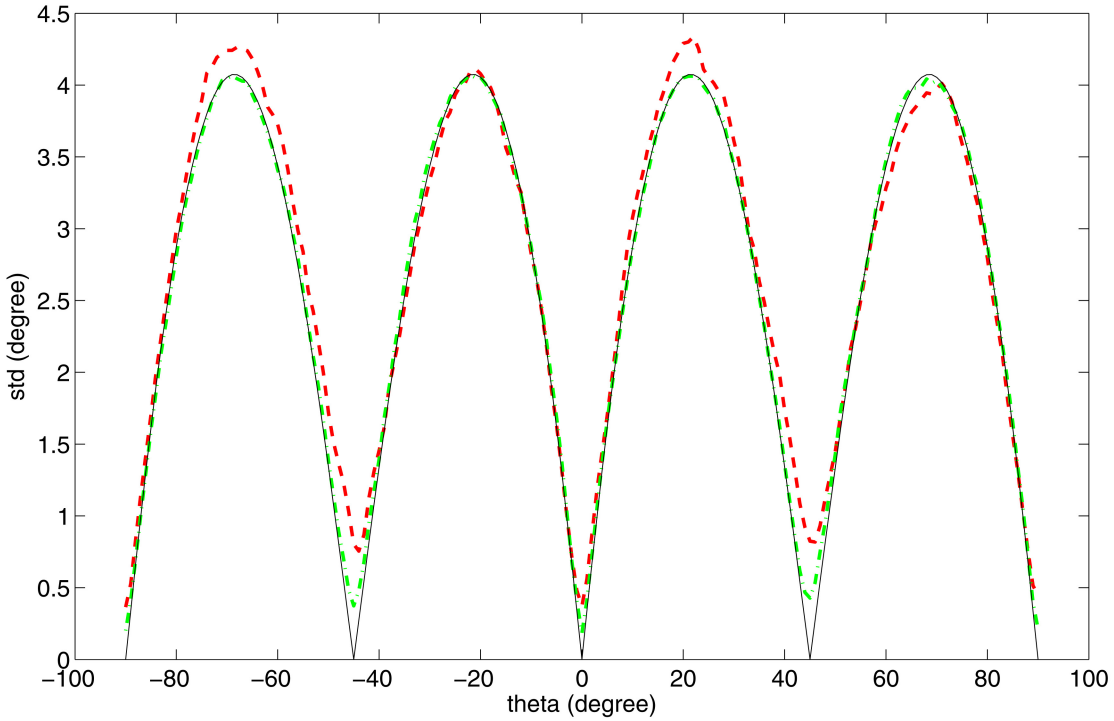

Fig. 6. Phase estimation standard deviation error of APD when N = 1024 (dashed line), 4096 (dash-dotted line) and theoretical value when $N \to \infty$ (solid line) as SNR = 20 dB, using 100 Monte Carlo simulation trials.

f_s = 4.096 MHz, as shown in Fig. 6. In low SNR cases the deviation reduces if N is sufficiently large, as illustrated in Fig. 7. This is consistent with the result of the noise effect on the periodic phase detector characteristic when the SNR is sufficiently low [16, 17, Sect. 6.5]. Hence for applications in low SNR cases, high accuracy carrier phase estimation can be achieved by using a 1-bit APD with sufficient samples. However for high SNR cases, significant deviation exists. In the next section a novel 1-bit phase discriminator is proposed to achieve high accuracy phase estimation in high SNR cases.

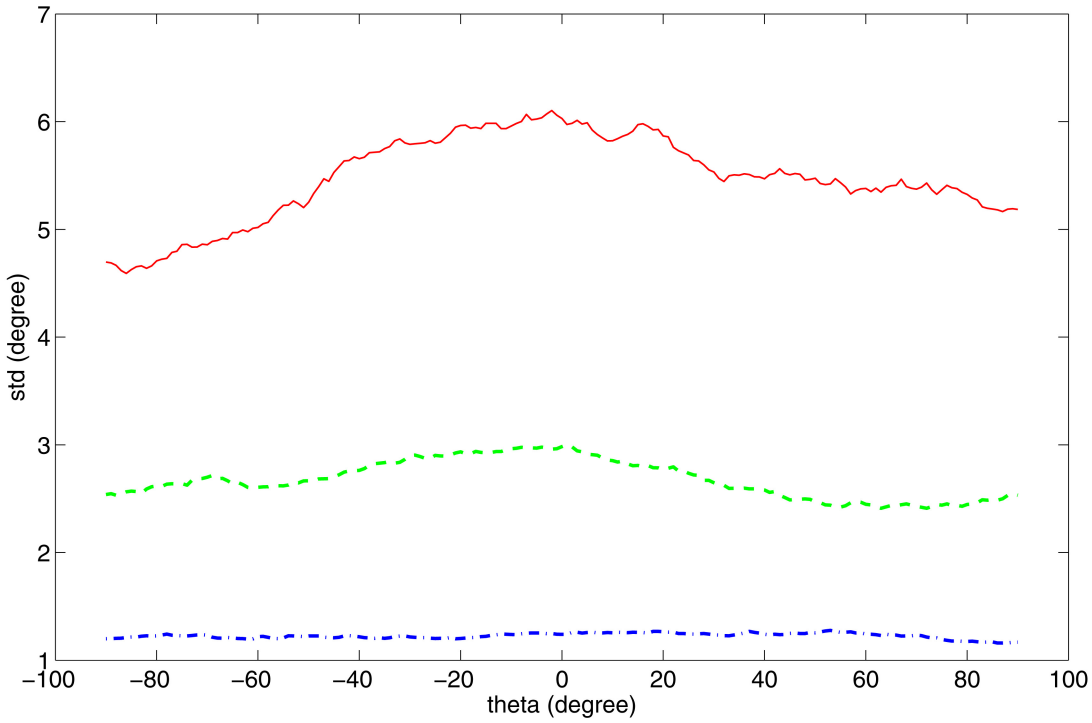

Fig. 7. Phase estimation standard deviation error of APD when $N = 20480$ (solid line), 81920 (dashed line), and 409600 (dash-dotted line) when SNR = −20 dB using 100 Monte Carlo simulation trials.

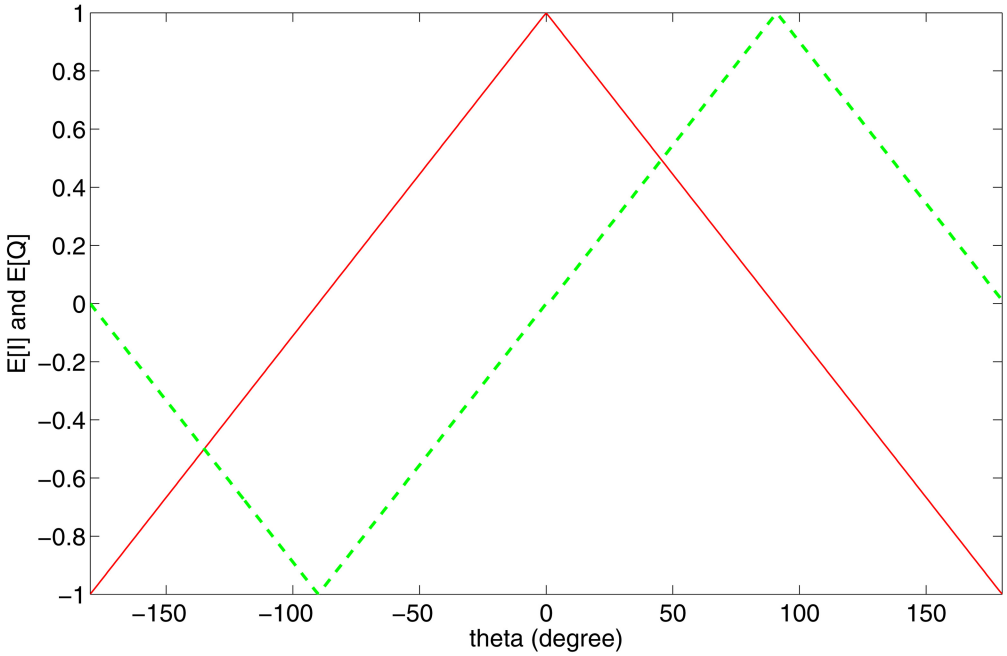

Fig. 8. Expected values $E[\mathbf{I}]$ (solid line) and $E[\mathbf{Q}]$ (dashed line) in noiseless cases.

V. NOISE-BALANCED DIGITAL PHASE DISCRIMINATOR

First, the noiseless case of $E[\mathbf{I}]$ and of $E[\mathbf{Q}]$ are considered, as shown in Fig. 8. The linear curve of $E[\mathbf{I}]$ is given by

$$E[\mathbf{I}] = E[\mathbf{I}]_{\max}\left(1 - \frac{2}{\pi}\cdot|\theta|\right). \tag{33}$$

Since $E[\mathbf{I}]_{\max} = 1$, we can derive θ from (33) given by

$$|\theta| = \frac{\pi}{2}\cdot(1 - E[\mathbf{I}]). \tag{34}$$

From Fig. 8 we further find

$$\operatorname{sgn}(\theta) = \operatorname{sgn}(E[\mathbf{Q}]). \tag{35}$$

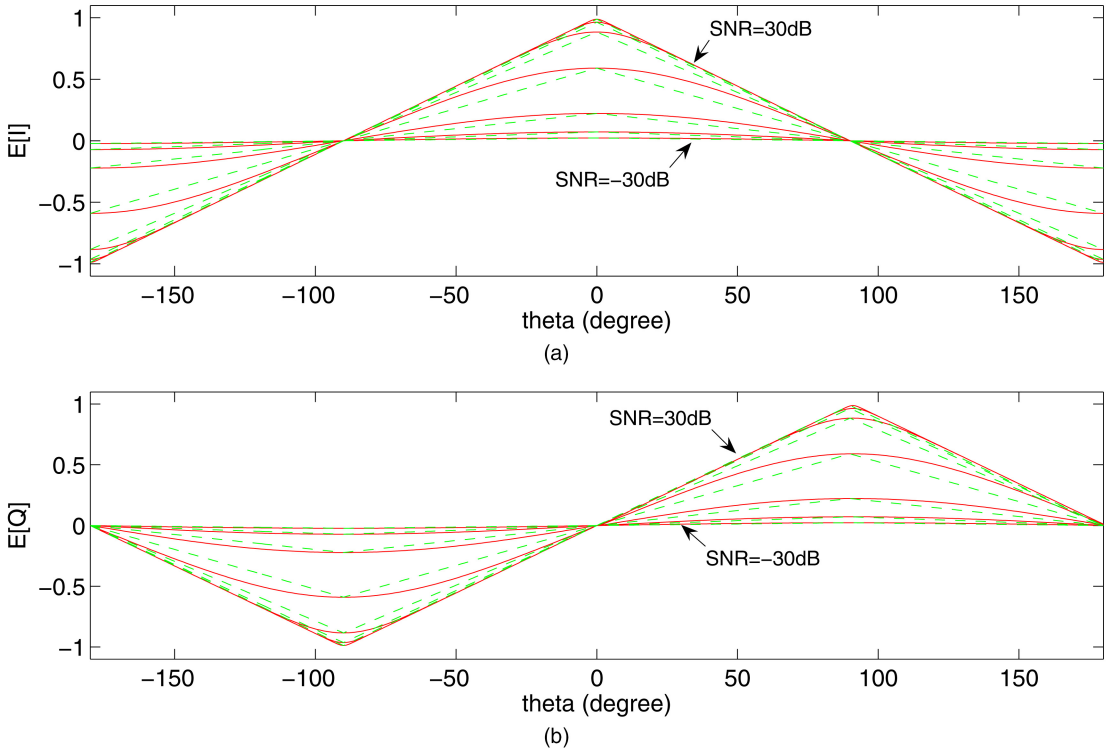

Fig. 9. Expected values of (a) $E[\mathbf{I}]$ (solid line), its linear approximations (dashed line), and (b) $E[\mathbf{Q}]$ when SNR = −30 dB, −20 dB…30 dB.

Hence the polarity ambiguity of θ in (34) can be resolved, and thus

$$\theta = \text{sgn}(E[\mathbf{Q}]) \cdot \frac{\pi}{2} \cdot (1 - E[\mathbf{I}]). \tag{36}$$

Equation (36) tells us that θ can be derived by using $E[\mathbf{I}]$ and $E[\mathbf{Q}]$ under noiseless environments.

In noisy cases we can still utilize (33) to approximate $E[\mathbf{I}]$ (dashed line) with modified $E[\mathbf{I}]_{\max}$ in (21), as shown in Fig. 9(a). Hence the phase can be approximated using (33), given by

$$|\theta| \approx \frac{\pi}{2} \cdot \left(1 - \frac{E[\mathbf{I}]}{E[\mathbf{I}]_{\max}}\right). \tag{37}$$

From Fig. 9(b) the polarity ambiguity of the phase estimate can also be resolved using the sign of $E[\mathbf{Q}]$. Hence the estimate of θ is given by

$$\theta \approx \text{sgn}(E[\mathbf{Q}]) \cdot \frac{\pi}{2} \cdot \left(1 - \frac{E[\mathbf{I}]}{E[\mathbf{I}]_{\max}}\right). \tag{38}$$

Next, from (21), $E[\mathbf{I}]_{\max}$ is a function of the SNR, which is unknown in many realistic situations. Here we propose an approximation for $E[\mathbf{I}]_{\max}$ in the following.

When SNR $\to \infty$, from Fig. 8, we find that

$$|E[\mathbf{I}]| + |E[\mathbf{Q}]| = E[\mathbf{I}]_{\max} \qquad \text{for} \quad \theta \in [-\pi, \pi). \tag{39}$$

Hence we make the linear approximation for high SNR cases as

$$E[\mathbf{I}]_{\max} \approx |E[\mathbf{I}]| + |E[\mathbf{Q}]| \qquad \text{for} \quad \theta \in [-\pi, \pi). \tag{40}$$

In order to verify this, we plot $|E[\mathbf{I}]| + |E[\mathbf{Q}]|$, as shown in Fig. 10. From Fig. 10 the approximation also holds well in low-SNR cases.

Finally, by inserting (40) into (38), we attain a phase discriminator independent of the SNR, given by

$$\theta \approx \text{sgn}(E[\mathbf{Q}]) \cdot \frac{\pi}{2} \cdot \left(1 - \frac{E[\mathbf{I}]}{|E[\mathbf{I}]| + |E[\mathbf{Q}]|}\right). \tag{41}$$

In practice, as we have enough samples, i.e., $N \to \infty$, from the definitions of $\mathbf{I}$ and $\mathbf{Q}$, we have $\mathbf{I} \to E[\mathbf{I}]$ and $\mathbf{Q} \to E[\mathbf{Q}]$, respectively. Hence the phase can be estimated by

$$\hat{\theta}_{\text{NBDPD}} = \text{sgn}(\mathbf{Q}) \cdot \frac{\pi}{2} \cdot \left(1 - \frac{\mathbf{I}}{|\mathbf{I}| + |\mathbf{Q}|}\right). \tag{42}$$

This phase discriminator is called NB-DPD since the affect of noise is approximately balanced in the factor $|\mathbf{I}| + |\mathbf{Q}|$, which is the key for the NB-DPD to achieve high accuracy in high-SNR cases. Note that the NB-DPD does not require knowledge of the SNR and that the computation is less than the APD.

VI. ASYMPTOTIC DEVIATION OF NB-DPD

A. Noiseless Environments

In noiseless environments, from Fig. 8, we have

$$|E[\mathbf{I}]| + |E[\mathbf{Q}]| = 1. \tag{43}$$

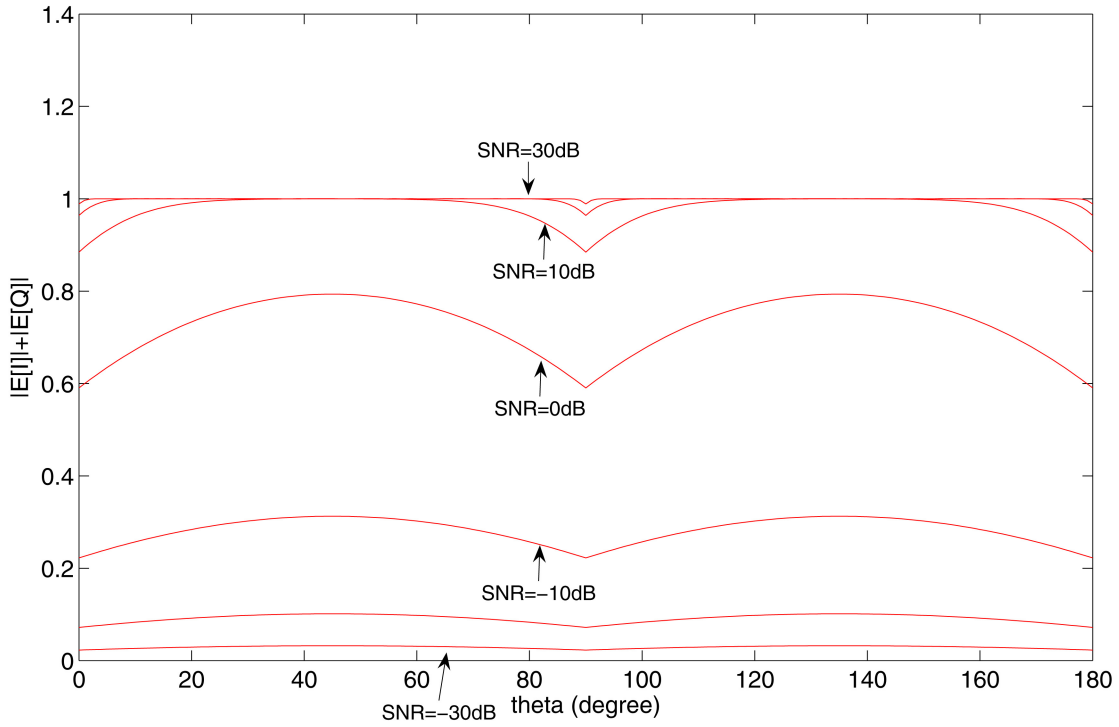

Fig. 10. $|E[\mathbf{I}]| + |E[\mathbf{Q}]|$ when SNR = −30 dB, −20 dB…30 dB.

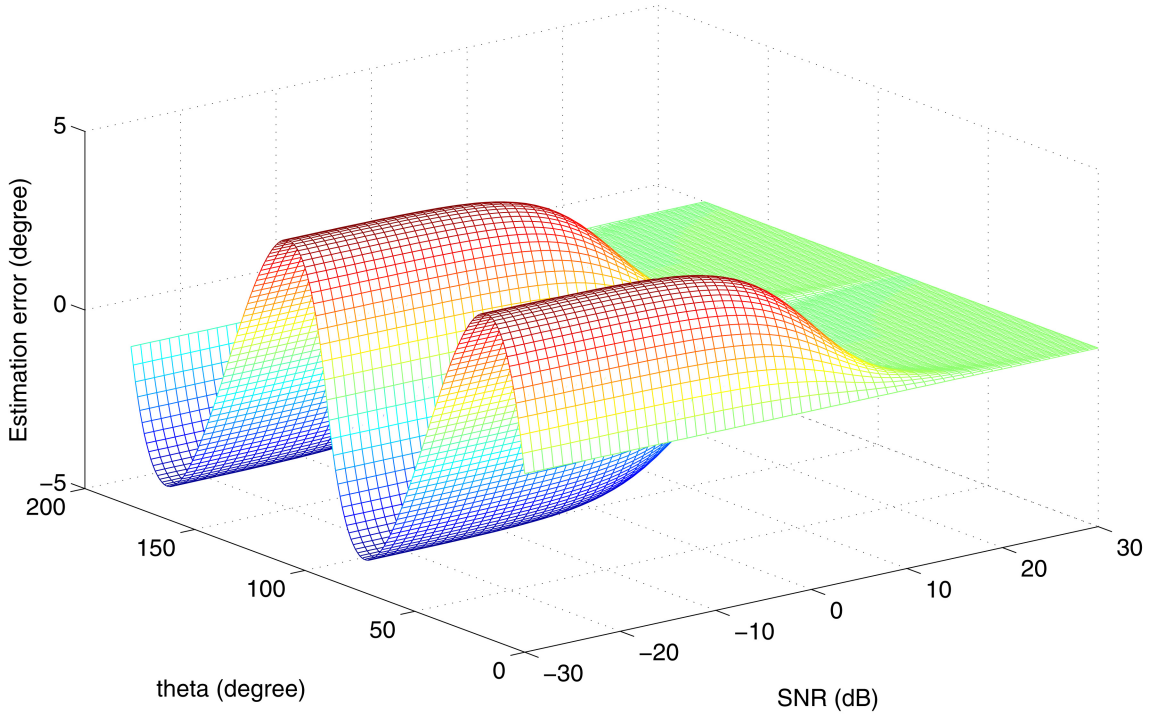

Fig. 11. Asymptotic deviation $\hat{\theta}_{\text{NBDPD}} - \theta$.

By combining (43) and (41), we have

$$\hat{\theta}_{\text{NBDPD}} = \text{sgn}[E[\mathbf{Q}]] \cdot \frac{\pi}{2} \cdot (1 - E[\mathbf{I}]) \tag{44}$$

which is equivalent to the DPD proposed in [12]. Hence the NB-DPD inherits the high-accuracy properties of the DPD in noiseless or high-SNR cases.

B. Noisy Environments

From (20), (23), (40), and (41), the asymptotic deviation of the NB-DPD is provided in Fig. 11. Obviously the NB-DPD achieves high accuracy phase estimation in high-SNR cases. This is consistent with the results in Section VI-A. On the other hand the estimation error gets bigger in low-SNR cases.

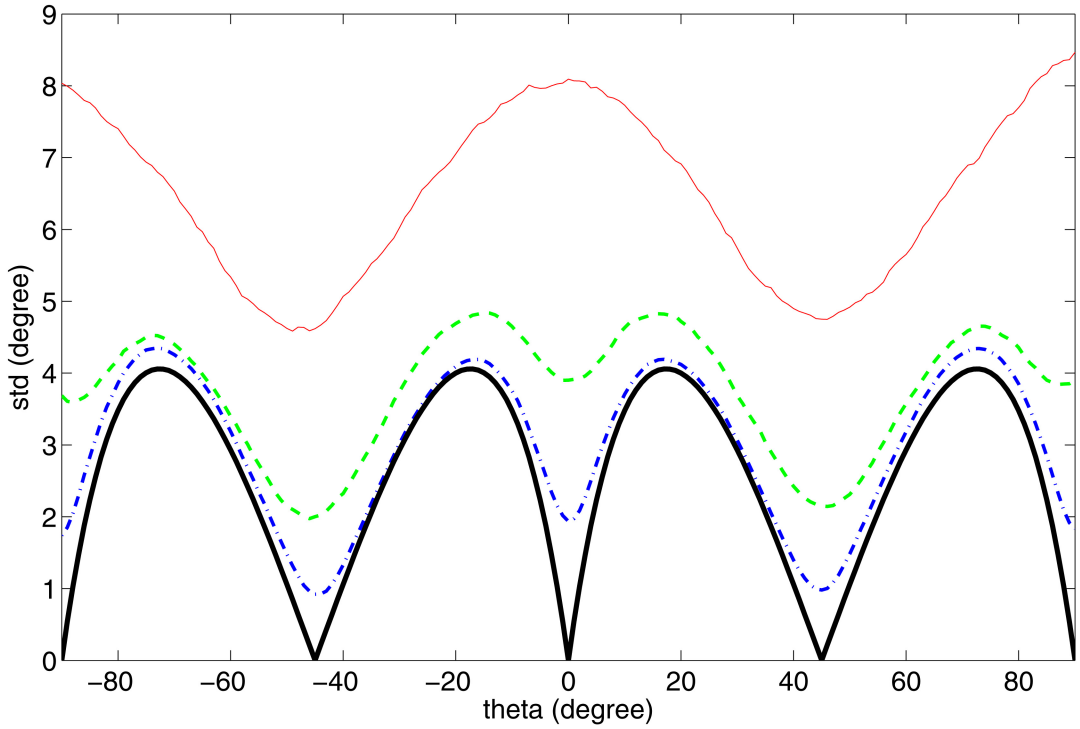

Fig. 12. Phase estimation standard deviation error of NB-DPD when $N = 20480$ (solid line), 81920 (dashed line), and 409600 (dash-dotted line), with absolute cross-section (bold solid line) of Fig. 11, when SNR = −20 dB using 100 Monte Carlo simulation trials, where $f_c = 15.42$ MHz and $f_s = 4.096$ MHz.

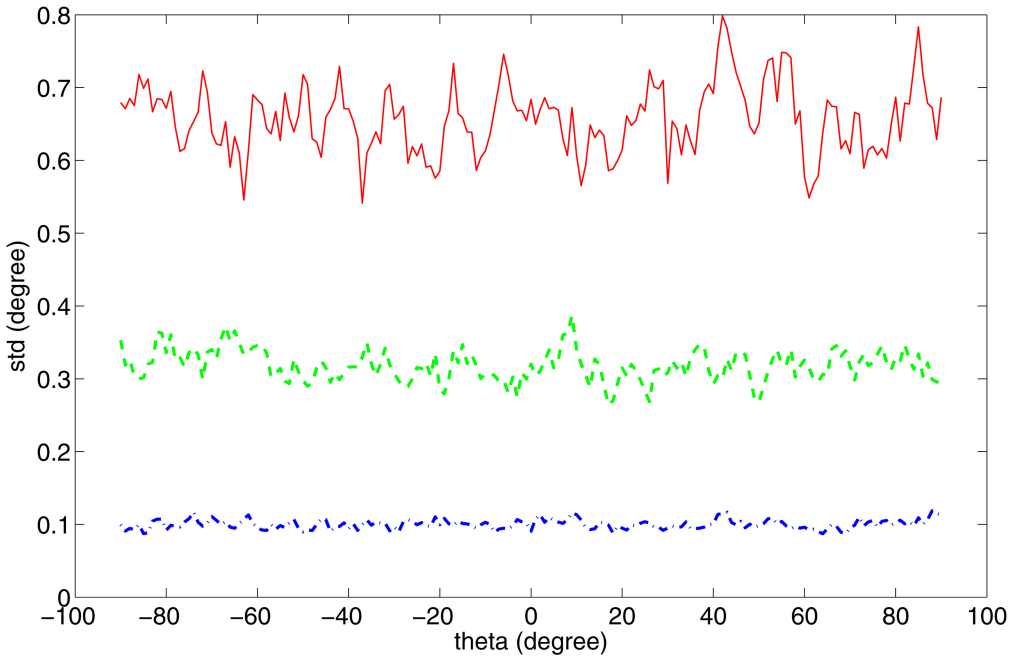

Fig. 13. Phase estimation standard deviation error of NB-DPD when $N = 1024$ (solid line), 4096 (dashed line), and 40960 (dash-dotted line), when SNR = 20 dB using 100 Monte Carlo simulation trials, where $f_c = 15.42$ MHz and $f_s = 4.096$ MHz.

As the SNR becomes extremely low, maximum estimation errors occur at 17.4°, 72.6°, 107.4°, and 162.6°, while the minimum occur at 0°, 45°, 90°, and 135°. The maximum deviation is about ±4°, and the minimum deviation is zero. The analysis of searching local extrema and the associated positions are provided in Appendix II. Note that the positions of local extrema depend on the SNR and that they may slightly vary in low-SNR cases. From Fig. 11 the deviation exists even if the sampling count $N \to \infty$. In order to obtain more insight, the estimation performance with SNR = −20 dB is provided in Fig. 12, where a Monte Carlo simulation is used for 100 trials. From Fig. 12 the simulated results

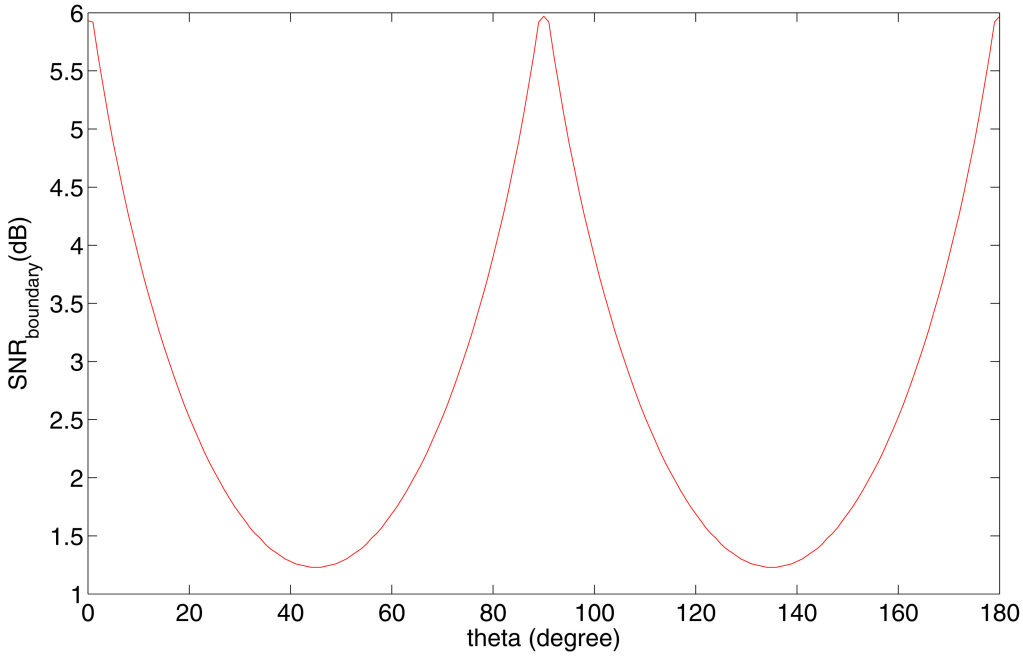

Fig. 14. Phase estimation performance transition between NB-DPD and APD.

approach the theoretical estimation deviation error derived in (41) as N increases. On the other hand when SNR = 20 dB, the deviation is reduced, as illustrated in Fig. 13. These results are consistent with the LLN since $\mathbf{I} \to E[\mathbf{I}]$ and $\mathbf{Q} \to E[\mathbf{Q}]$ when $N \to \infty$, as shown in (28)–(31). Hence in high-SNR cases, a high-accuracy carrier phase estimation can be achieved by using the NB-DPD. Note that comparing Fig. 13 with Fig. 12, convergence is achieved by using many fewer samples in high-SNR cases.

As we compare Fig. 5 with Fig. 11, it is interesting to see the complementary performance between the NB-DPD and the APD, which reveals the cooperative potential for various applications. Furthermore it is worth comparing the performance difference between the NB-DPD and the APD in "mid-SNR" (SNR is neither high nor low) cases. First let δ_{APD} and δ_{NBDPD} be the asymptotic deviations of APD and NB-DPD given by

$$\delta_{\text{APD}} = \hat{\theta}_{\text{APD}} - \theta \tag{45}$$

$$\delta_{\text{NBDPD}} = \hat{\theta}_{\text{NBDPD}} - \theta \tag{46}$$

when $N \to \infty$. In (45)–(46), δ_{APD} and δ_{NBDPD} are functions of the SNR and can be derived from (20), (23), (24), and (42). Because of the nonlinearity of the arctangent function and the complexity of the double integral, the analysis of performance difference seems intractable when the SNR is neither high nor low. Using the numerical method, the performance "boundary" between the NB-DPD and the APD is provided in Fig. 14, where the pair $(\theta, \text{SNR}_{\text{boundary}})$ satisfies that

$$\delta_{\text{NBDPD}} = \delta_{\text{APD}}. \tag{47}$$

Thus when $\text{SNR} > \text{SNR}_{\text{boundary}}$, the estimation error of $\hat{\theta}_{\text{NBDPD}}$ is less than that of $\hat{\theta}_{\text{APD}}$. As we take the averages of δ_{APD} and δ_{NBDPD} over $\theta \in [-\pi, \pi)$, the average absolute estimation error of both cases is obtained numerically, as shown in Fig. 15. The intersection point suggests that the threshold SNR can be set at 2.6 dB and can be used to determine whether the NB-DPD or the APD should be adopted according to the respective application. When SNR > 2.6 dB the NB-DPD should be chosen; otherwise, the APD should be adopted.

VII. CONVERGENCE OF I AND Q

As we investigate the convergence of the estimates in (28)–(32), two driving factors are considered: phase ambiguity determined by P and variance determined by M.

First for phase ambiguity the resolution is $2\pi/P$, and the ambiguity reduces as P increases. Since P is determined by the carrier frequency and the sampling rate, as shown in (8), a proper selection of these two parameters and of the integration time (number of samples N) is important.

Next for variance reduction the noise and quantization effects are reduced as M increases. Since our approach considers the dependence between neighboring quantized samples, it is not tractable to derive the probability distribution of the APD or the NB-DPD directly. However it is obvious that the convergence is determined by the convergence of $\mathbf{I}$ and $\mathbf{Q}$. Hence we derive the variances of $\mathbf{I}$ and $\mathbf{Q}$ as follows. Consider the inphase correlator components in the noiseless case, given by

$$I_{o,n} = \text{sgn}[\sin(\phi_n + \theta)] \cdot \text{sgn}[\sin \phi_n] \tag{48}$$

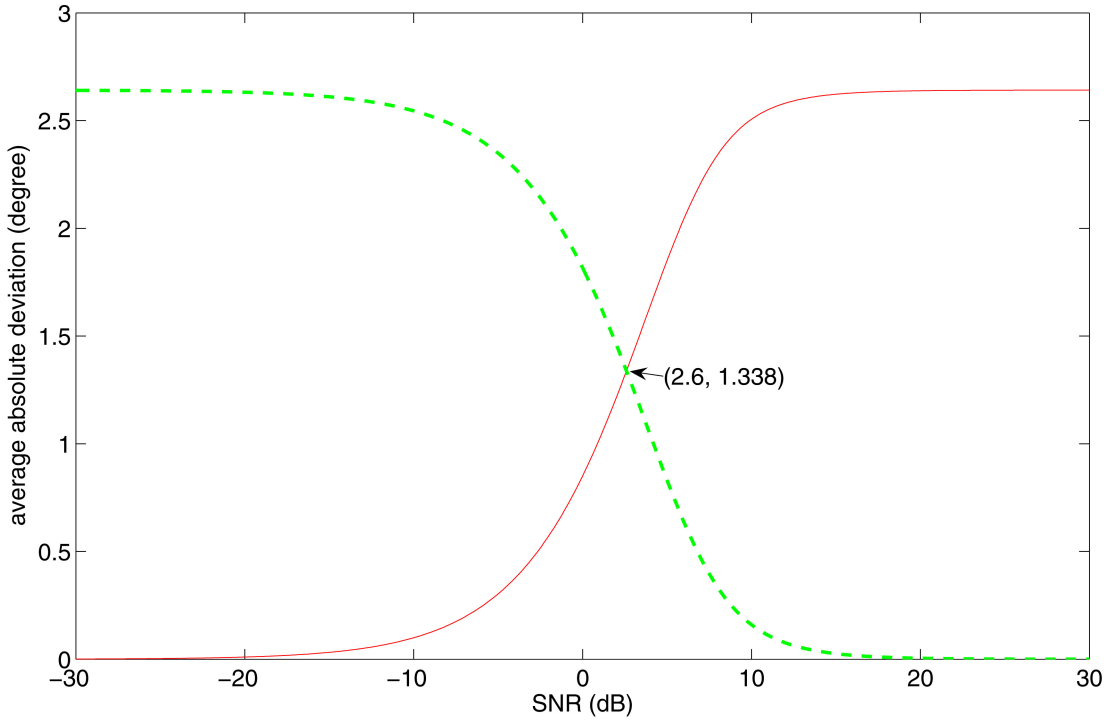

Fig. 15. Average asymptotic deviation of APD (solid line) and NB-DPD (dashed line).

where $n = 0, 1 \ldots P-1$. From (11)–(15) we have

$$\Pr(\mathbf{I}_n = I_{o,n}) = 1 - \alpha_n$$
$$\Pr(\mathbf{I}_n = -I_{o,n}) = \alpha_n$$

where

$$\alpha_n = \mathrm{G}(\gamma|\sin(\phi_n + \theta)|). \tag{49}$$

Thus the variance of $\mathbf{I}_n$ is given by

$$\begin{aligned}\sigma_n^2 &= E[\mathbf{I}_n^2] - E[\mathbf{I}_n]^2 \\ &= (1-\alpha_n)I_{o,n}^2 + \alpha_n(-I_{o,n})^2 - [(1-\alpha_n)I_{o,n} - \alpha_n I_{o,n}]^2 \\ &= 4\alpha_n(1-\alpha_n)\end{aligned} \tag{50}$$

since $I_{o,n}^2 = 1$. Hence for each group of IID samples $\mathbf{I}_k, \mathbf{I}_{k+P} \ldots \mathbf{I}_{k+(M-1)P}$, the group average in (28) approaches its ensemble average with variance $4\alpha_n(1-\alpha_n)/M$, which vanishes as $M \to \infty$. From (29) it applies to quadrature-channel as well.

From above, increasing P and M can reduce the phase ambiguity and the variance, respectively. The price is the computation and the complexity. Hence it is critical to select proper P and M in order to achieve the desired high accuracy efficiently.

VIII. DISCUSSION AND CONCLUSIONS

Asymptotic deviation of the traditional APD is provided in (20), (23), and (32), as shown in Fig. 5, for 1-bit processing receivers. As sufficient samples are obtained (N is sufficiently large), the APD can attain high accuracy in low-SNR cases. However in high-SNR cases, the APD may have an estimation deviation up to 4.1°, and thus a novel phase discriminator NB-DPD is proposed in (42). The NB-DPD is developed using linear approximation and provides a better estimate than APD does in high-SNR cases, as shown in Fig. 11. The extrema of asymptotic deviation for the APD in high-SNR cases and the NB-DPD in low-SNR cases are derived analytically in Appendix I and in Appendix II, respectively. In addition the threshold SNR 2.6 dB is derived numerically, as shown in Fig. 15, to select either the NB-DPD or the APD accordingly.

It is worth mentioning that the proposed approach that derives the asymptotic deviation in Section III and Section IV works even though the neighboring quantized samples are dependent (the proof is provided in Appendix III). This dependence may be caused by the dependence of neighboring environmental noise components or by the dependence of quantization noise on signal. In our approach we only require the very general condition that a noise component sample $\mathbf{u}_n$ is independent of $\mathbf{u}_{n+j}$ if $j \geq P$ since P is typically large. Note that the non-Gaussian noise can be incorporated in our approach and that, in (13) the G-function can be replaced by the tail probability of the noise distribution.

Finally, for data-free applications such as pilot channel, the proposed algorithm can be readily used. For data-bearing channels, the algorithm is adopted in tracking loop after data is removed. In the future it will be interesting to further explore the effects of sampling, quantization, and noise and signal waveform (separately and jointly) on asymptotic

performance of carrier phase discriminators. This would be our next step.

APPENDIX I

First consider noiseless cases, i.e., SNR $\to \infty$, and for simplicity, assume $0 \le \theta < \pi/2$. From Fig. 8 $E[\mathbf{I}]$ and $E[\mathbf{Q}]$ are given by

$$E[\mathbf{I}] = 1 - \frac{2\theta}{\pi} \tag{51}$$

$$E[\mathbf{Q}] = \frac{2\theta}{\pi}. \tag{52}$$

Hence the deviation of the APD is given by

$$\begin{aligned}\delta_{\text{APD}} &= \hat{\theta}_{\text{APD}} - \theta \\ &= \tan^{-1}\frac{\frac{2\theta}{\pi}}{1-\frac{2\theta}{\pi}} - \theta \\ &= \tan^{-1}\frac{2\theta}{\pi - 2\theta} - \theta.\end{aligned} \tag{53}$$

The extrema can be derived by taking the derivative of (53), given by

$$\max_{\theta} \delta_{\text{APD}} \Rightarrow \frac{d\delta_{\text{APD}}}{d\theta} = 0.$$

Then we have

$$\begin{aligned}&\frac{2(\pi-2\theta)+4\theta}{(\pi-2\theta)^2}\cdot\frac{1}{\left(\frac{2\theta}{\pi-2\theta}\right)^2+1} - 1 = 0 \\ \Rightarrow\quad & 8\theta^2 - 4\pi\theta + \pi^2 - 2\pi = 0 \\ \Rightarrow\quad & \theta = \frac{\pi \pm \sqrt{4\pi - \pi^2}}{4} \\ & = 0.375 \text{ rad } (21.5^\circ) \text{ or } 1.196 \text{ rad } (68.5^\circ).\end{aligned} \tag{54}$$

By inserting (54) into (53), we obtain the extreme deviations $\pm 4.1^\circ$. Note that, from (53), $\delta_{\text{APD}} = 0$ when $\theta = 0^\circ$ or 45°. Similarly we can obtain the location of extreme values when $\pi/2 \le \theta < \pi$: 111.5° and 158.5°, and $\delta_{\text{APD}} = 0$ when $\theta = 90^\circ$ or 135°.

APPENDIX II

Since the error function has Taylor expansion, given by

$$\text{erf}(x) = \frac{2}{\sqrt{\pi}}\sum_{n=0}^{\infty}\frac{(-1)^n x^{2n+1}}{n!(2n+1)} \tag{55}$$

the G-function can be approximated by

$$\begin{aligned}\text{G}(x) &= \frac{1}{2} - \frac{1}{2}\text{erf}\left(\frac{x}{\sqrt{2}}\right) \\ &\approx \frac{1}{2} - \frac{x}{\sqrt{2\pi}}\end{aligned} \tag{56}$$

when $x \to 0$. Hence when SNR $\ll 1$, (20) can be approximated by

$$\begin{aligned}E[\mathbf{I}] &\approx \frac{1}{\pi}\cdot\left\{\int_{\pi+\theta}^{2\pi+\theta}\frac{1}{2} - \frac{\gamma\sin\psi}{\sqrt{2\pi}}d\psi - \int_{\theta}^{\pi+\theta}\frac{1}{2} - \frac{\gamma\sin\psi}{\sqrt{2\pi}}d\psi\right\} \\ &= \frac{2\sqrt{2}\gamma}{\pi^{3/2}}\cos\theta \\ &= h\cos\theta\end{aligned} \tag{57}$$

where $h = 2\sqrt{2}\gamma/\pi^{3/2}$. Similarly (23) can be approximated by

$$E[\mathbf{Q}] \approx h\sin\theta \tag{58}$$

when SNR $\ll 1$. Now consider the deviation of the NB-DPD when $0 \le \theta < \pi/2$, given by

$$\begin{aligned}\delta_{\text{NBDPD}} &= \hat{\theta}_{\text{NBDPD}} - \theta \\ &= \text{sgn}(E[\mathbf{Q}])\cdot\frac{\pi}{2}\cdot\left(1 - \frac{E[\mathbf{I}]}{|E[\mathbf{I}]| + |E[\mathbf{Q}]|}\right) - \theta \\ &= \frac{\pi}{2}\left(1 - \frac{\cos\theta}{\cos\theta + \sin\theta}\right) - \theta.\end{aligned} \tag{59}$$

The extrema can be derived by taking the derivative of (59) given by

$$\max_{\theta} \delta_{\text{NBDPD}} \Rightarrow \frac{d\delta_{\text{NBDPD}}}{d\theta} = 0.$$

Then we have

$$\begin{aligned}&\frac{\pi}{2}\cdot\frac{\sin\theta(\cos\theta+\sin\theta) + \cos\theta(\cos\theta - \sin\theta)}{(\cos\theta+\sin\theta)^2} - 1 = 0 \\ \Rightarrow\quad & (\cos\theta + \sin\theta)^2 = \frac{\pi}{2} \\ \Rightarrow\quad & \theta = \frac{1}{2}\sin^{-1}\left(\frac{\pi}{2} - 1\right) \text{ or } \frac{\pi}{2} - \frac{1}{2}\sin^{-1}\left(\frac{\pi}{2} - 1\right) \\ \Rightarrow\quad & \theta = 0.3037 \text{ rad } (17.4^\circ) \text{ or } 1.2671 \text{ rad } (72.6^\circ).\end{aligned} \tag{60}$$

By inserting (60) into (59), we obtain the extreme deviations $\pm 4^\circ$. Note that, from (59), $\delta_{\text{NBDPD}} = 0$ when $\theta = 0^\circ$ or 45°. Similarly we can obtain the location of the extreme values when $\pi/2 \le \theta < \pi$: 107.4° and 162.6°, and $\delta_{\text{APD}} = 0$ when $\theta = 90^\circ$ or 135°.

APPENDIX III

Without loss of generality we consider two beginning consecutive data in each group of P samples. First from the assumption in Section IV, noise components $\mathbf{u}_n$ and $\mathbf{u}_{n+j}$ are independent when $j \ge P$. Hence $\mathbf{I}_0, \mathbf{I}_P \mathbf{I}_{2P} \ldots \mathbf{I}_{MP}$ are IID Gaussian random variables, and $\mathbf{I}_1, \mathbf{I}_{P+1}\mathbf{I}_{2P+1}\ldots\mathbf{I}_{MP+1}$ are IID Gaussian random variables.

Suppose that the consecutive data are correlated, i.e.,

$$E[\mathbf{I}_{mP}\mathbf{I}_{mP+1}] = E[\mathbf{I}_{mP}]E[\mathbf{I}_{mP+1}] + A_m \tag{61}$$

where $A_m \neq 0$. We want to prove that when $M \to \infty$, $\mathbf{X}$ and $\mathbf{Y}$ are independent, where

$$\mathbf{X} = \frac{1}{M}\sum_{m=0}^{M-1}\mathbf{I}_{mP}$$

$$\mathbf{Y} = \frac{1}{M}\sum_{m=0}^{M-1}\mathbf{I}_{mP+1}.$$

Next the cross-correlation between $\mathbf{X}$ and $\mathbf{Y}$ is given by

$$\begin{aligned}
E[\mathbf{XY}] &= E\left[\frac{1}{M}\sum_{m=0}^{M-1}\mathbf{I}_{mP}\cdot\frac{1}{M}\sum_{n=0}^{M-1}\mathbf{I}_{nP+1}\right] \\
&= \frac{1}{M^2}E\left[\sum_{m=0}^{M-1}\sum_{n=0}^{M-1}\mathbf{I}_{mP}\mathbf{I}_{nP+1}\right] \\
&= \frac{1}{M^2}\sum_{m=0}^{M-1}E[\mathbf{I}_{mP}\mathbf{I}_{mP+1}] + \frac{1}{M^2}\sum_{m=0}^{M-1}\sum_{n=0,n\neq m}^{M-1}E[\mathbf{I}_{mP}\mathbf{I}_{nP+1}] \\
&= \frac{1}{M^2}\sum_{m=0}^{M-1}E[\mathbf{I}_{mP}]E[\mathbf{I}_{mP+1}] + \frac{1}{M^2}\sum_{m=0}^{M-1}A_m \\
&\quad + \frac{1}{M^2}\sum_{m=0}^{M-1}\sum_{n=0,n\neq m}^{M-1}E[\mathbf{I}_{mP}]E[\mathbf{I}_{nP+1}] \qquad (62)
\end{aligned}$$

since $\mathbf{I}_{mP}$ and $\mathbf{I}_{nP+1}$ are reasonably assumed to be uncorrelated when $m \neq n$. In addition the 2nd term of (62) vanishes as $M \to \infty$. Hence (62) can be rewritten as

$$\begin{aligned}
E[\mathbf{XY}] &= \frac{1}{M^2}\sum_{m=0}^{M-1}E[\mathbf{I}_{mP}]E[\mathbf{I}_{mP+1}] \\
&\quad + \frac{1}{M^2}\sum_{m=0}^{M-1}\sum_{n=0,n\neq m}^{M-1}E[\mathbf{I}_{mP}]E[\mathbf{I}_{nP+1}] \\
&= E[\mathbf{X}]E[\mathbf{Y}].
\end{aligned}$$

Since $\mathbf{X}$ and $\mathbf{Y}$ are Gaussian, the uncorrelation implies independence. Thus the proposed approach deriving asymptotic deviation in Section III and Section IV works even though the neighboring quantized samples are dependent.

REFERENCES

[1] Brown, A. and Wolt, B.
Digital L-band receiver architecture with direct RF sampling.
IEEE Position Location and Navigation Symposium, Las Vegas, NV, Apr. 11–15, 1994, pp. 209–216.

[2] Wu, P. H.
The optimal BPSK demodulator with a 1-bit A/D front-end.
Proceedings of the IEEE Military Communications Conference (MILCOM '98), vol. 3, Bedford, MA, Oct. 18–21, 1998, pp. 730–735.

[3] Figucia, R.
Advanced SCAMP'S demodulator design for performing evelope recovery from hard limited samples.
MILCOM '92, 1992, pp. 385–389.

[4] Parkinson, B. and Spilker, J.
Global Positioning System: Theory and Applications, vol. I. Reston, VA: AIAA, 1996.

[5] Chang, H.
Presampling filtering, sampling and quantization effects on the digital matched filter performance.
Proceedings of the International Telemetering Conference, San Diego, CA, Sept. 1982, pp. 889–915.

[6] Ledvina, B., et al.
A real-time GPS civilian L1/L2 software receiver.
Proceedings of ION GNSS 2004, Long Beach, CA, Sept. 21–24, 2004, pp. 986–1005.

[7] Proakis, J. G.
Digital Communications (3rd ed.).
New York: McGraw-Hill, 1995.

[8] Cohen, C.
Attitude determination using GPS.
Ph.D. dissertation, Dept. of Aeronautics and Astronautics, Stanford University, Stanford, CA, 1992.

[9] Rocken, C., et al.
COSMIC system description.
Special Issue of Terrestrial, Atmospheric and Oceanic Science, **11**, 1 (Mar. 2000), 21–52.

[10] Hajj, G., et al.
A technical description of atmospheric sounding by GPS occultation.
Journal of Atmospheric and Solar-Terrestrial Physics, **64** (2002), 451–469.

[11] Sykora, J. and Schober, R.
Multiplexing precoding scheme for STC-CPM with parametric phase discriminator IWM receiver.
Proceedings of the IEEE 19th International Symposium on Personal, Indoor and Mobile Radio Communications, Cannes, France, Sept. 15–18, 2008, pp. 1–6.

[12] Chang, C-F. and Kao, M-S.
High-accuracy carrier phase discriminator for one-bit quantized software-defined receivers.
IEEE Signal Processing Letters, **15** (2008), 397–400.

[13] Zhao, J., et al.
A robust digital phase discriminator in one-bit quantized software-defined receivers.
Proceedings of the 5th International Conference on Wireless Communications, Networking and Mobile Computing, Beijing, China, Sept. 24–26, 2009, pp. 24–26.

[14] Host-Madsen, A. and Handel, P.
Effects of sampling and quantization on single-tone frequency estimation.
IEEE Transactions on Signal Processing, **48**, 3 (Mar. 2000), 650–662.

[15] Andersson, T., Skoglund, M., and Händel, P.
Frequency estimation by 1-bit quantization and table look-up processing.
Proceedings of the European Signal Processing Conference (EUSIPCO-2000), Tampere, Finland, Sept. 5–8, 2000, pp. 1807–1810.

[16] Pouzet, A. H.
Characteristics of phase detector in the presence of noise.
Proceedings of the International Telemeter Conference, vol. 8, Los Angeles, CA, 1972, pp. 818–828.

[17] Gardner, F. M.
Phaselock Techniques (2nd ed.).
Hoboken, NJ: Wiley, 1979.

Chieh-Fu Chang received his Ph.D. in electrical and computer engineering from Purdue University, West Lafayette, IN.

He is currently an associate researcher at the Electrical Engineering Division of the National Space Organization (NSPO) in Taiwan. His current research interests include digital receivers, signal processing, satellite communications, and remote sensing instrument.

Ru-Muh Yang is an associate researcher in the Satellite Operation and Control (SOC) Division of the National Space Organization (NSPO) in Taiwan. He is responsible for the development and maintenance of the NSPO ground stations. His current research interests include software-defined GNSS receiver and satellite communications.

Ming-Seng Kao holds a Ph.D. in electrical engineering.

He is a professor in the Department of Communication Engineering at the National Chiao-Tung University, Taiwan. His current research interests include digital receivers, communications, coding, and optics.